

TEMPERATURE STRESSES IN A PACKET OF STRIPS PRODUCED FROM A MELT BY THE STEPANOV METHOD

A. V. Borodin, A. V. Zhdanov,
L. P. Nikolaeva, I. S. Pet'kov, and
L. P. Chupyatova

UDC 536.421

The authors suggest a mathematical model for describing thermoelastic stresses that appear during the growth of a packet of crystal strips that are in the state of radiation heat exchange with each other. It is assumed that the side surfaces of the strips are diffusely gray. The behavior of the stresses in the strips of the packet is investigated as a function of the pulling speed, the length of the grown strips, the distance between the shapers, their thickness, and the temperature of external shields.

Introduction. The technology of packet growth of profiled crystals by the Stepanov method makes it possible to increase the productivity substantially and to decrease expenditures of electric energy, water, and expendable materials. However, this process of growth requires a particularly careful selection of both the design of the shaper and the thermal field of the growth region. Experimental determination of these characteristics is very laborious and material consuming and ultimately offers no way of improving this process of growth.

Based on a mathematical simulation, we suggest that the process of packet growth be investigated with a view toward optimizing its characteristics for which the temperature stresses appearing in the packet strips would be minimum. The fulfillment of this requirement favors an increase in the productivity of the process and improvement of the quality of crystals produced. The mathematical model suggested includes: Navier–Stokes equations for determining the melt flow, a Stefan type problem for finding the temperature fields in the system crystal–melt and the crystallization front, Laplace equations which describe the profile curves of melt menisci, and an equation for the stress function. All of these equations were solved by the finite-element method, each being solved in its own permissible class of functions.

Formulation of the Problem. It is assumed that temperature stresses have no effect on the temperature distribution in the packet strips; in other words, the problem can be subdivided into two independent problems, namely: the heat problem and the problem proper of finding the temperature stresses.

In posing the heat problem for a packet of strips, we take into consideration the fact that it is sufficient to formulate this problem for one inner strip with small changes for two outer strips. This difference is just in the conditions of heat exchange between the side surfaces of the inner strips with each other and the outer strips with the environment. The scheme of the process of growth, the coordinate system, and the notation used are presented in Fig. 1. By subscripts 1 and 2 we denote the quantities that refer to the melt and the crystal, respectively. We will often use the same notation, but without containing the subscripts, and will imply that they refer to both the melt and the crystal. The temperature distribution $T_i(x, y)$, $i = 1, 2$, in the region of the melt and the crystal $D_1 \cup D_2$ is described by the following heat-conduction equations:

Institute of Solid-State Physics, Russian Academy of Sciences, Chernogolovka, Russia; email: zhdan@issp.ac.ru. Translated from *Inzhenerno-Fizicheskii Zhurnal*, Vol. 74, No. 3, pp. 106–112, May–June, 2001. Original article submitted March 16, 2000.

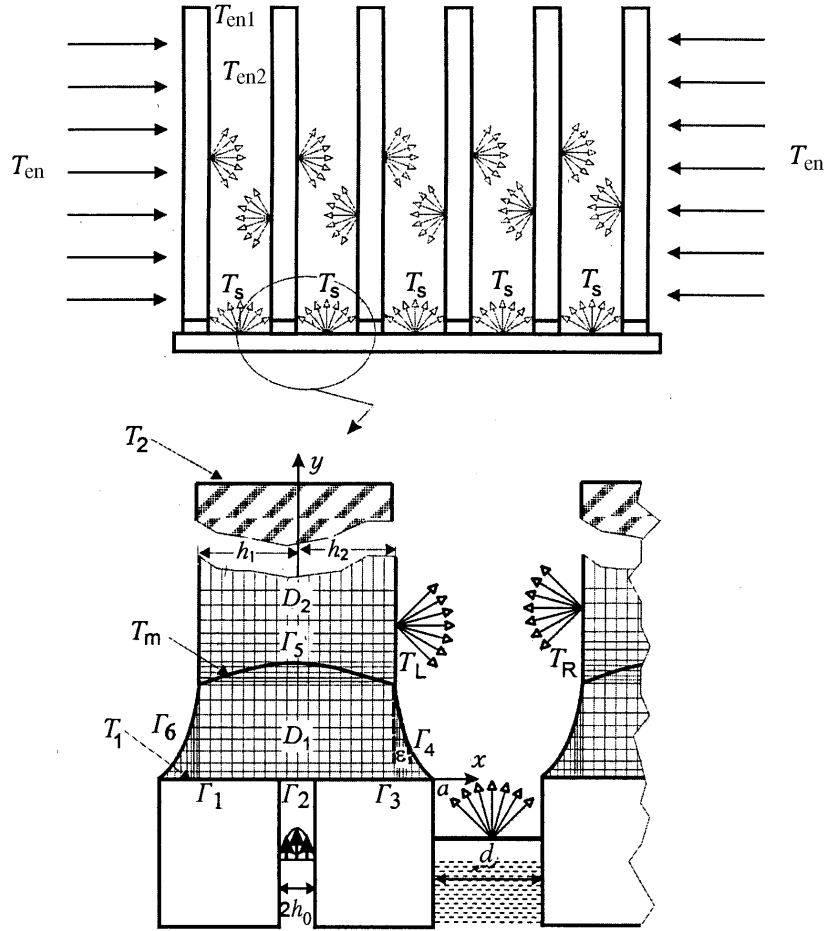


Fig. 1. Schematic diagram of the process of growth of crystal strips, the coordinate system, and the notation used.

$$\Delta T_i - \zeta_i (V_i, \nabla T_i) = 0, \quad (x, y) \in D_i, \quad \zeta_i = \frac{\rho_i c_i}{k_i}, \quad i = 1, 2, \quad (1)$$

where $V_1 = (u_1, v_1)$ is the distribution of the velocities of motion of the melt, which is determined below from the solution of the Navier-Stokes equations; $V_2 = (0, V_0)$ and V_0 is the pulling speed of the packet of strips.

On the crystallization front $H(x)$, the conditions for an interphase energy balance and the continuity condition for a temperature equal to the temperature of the melt T_m in passage through the crystallization front must be satisfied:

$$k_2 (n, \nabla T_2) - k_1 (n, \nabla T_1) = \rho_2 V_0 \Delta H_f (1 + H_x^2)^{1/2}, \quad (2)$$

$$T_1 [x, H(x)] = T_2 [x, H(x)] = T_m, \quad -h_1 \leq x \leq h_2, \quad y = H(x). \quad (3)$$

The heat from the melt and the crystal is transferred to the surrounding medium by both radiation and convection:

$$-k_i \frac{\partial T_i}{\partial n} = q_i, \quad i = 1, 2. \quad (4)$$

The explicit form of the flux densities q_i is different for the inner and outer strips of the packet. For the outer surfaces of the first and the last strip this form is

$$-k_i \frac{\partial T_i}{\partial \mathbf{n}} = h_{Gi} (T_i - T_{en}) + \sigma \varepsilon_i (T_i^A - T_{en}^A), \quad (5)$$

and for the inner strips it will be given below.

Moreover, we assign the temperatures at the upper ends of the strips, $T_2(x, l)$, and the temperatures of the melt at the ends of the shaper and at the exist of the capillary channel, $T_1(x, 0)$:

$$T_1(x, 0) = T_1^0(x), \quad -a \leq x \leq a, \quad T_2(x, l) = T_2^0(x), \quad -h_1 \leq x \leq h_2. \quad (6)$$

The profile curves of the melt menisci $f(y)$ satisfy the Young–Laplace capillary equation

$$\rho_2 g (y + H_{\text{eff}}) = \sigma_{\text{LG}} \frac{d}{dy} \left[\frac{df/dy}{(1 + (df/dy)^2)^{1/2}} \right] \quad (7)$$

with boundary conditions (for the right profile curve)

$$f(0) = a, \quad (8)$$

which corresponds to the meniscus being caught by the edge of the shaper, and

$$-\left. \frac{df}{dy} \right|_{y=H(h_2)} = \tan \varepsilon_0. \quad (9)$$

The second condition means that all the profile curves of the menisci make an angle equal to the growth angle ε_0 with the generatrix of the crystal surface. In a similar way, we also pose the problem for the left profile curve of the meniscus. They are related to each other by the common quantity H_{eff} .

To assign the boundary conditions in determining the velocity field $V_1 = (u_1, v_1)$ of the melt flow in the meniscus, we take into account the fact that the flow in the capillary channel is similar to that between two parallel plates.

The flow velocity of the melt in the meniscus V_1 and the pressure P satisfy the Navier–Stokes stationary equation and the following boundary conditions:

$$\mu \Delta V_1 + \rho_1 (V_1, \nabla) V_1 = \nabla P + F, \quad F = (0, -\rho_1 g), \quad \text{div } V_1 = 0. \quad (10)$$

On the portion of the boundary corresponding to the crystallization front $y = H(x)$ the conditions

$$V_{1n} = V_0 [1 + (H'_x)^2]^{1/2}, \quad V_{1\tau} = 0, \quad (11)$$

must be satisfied, which means that there is no flow along the crystallization front $H(x)$, while the projection of the normal velocity V_{1n} onto the y axis coincides with the pulling speed V_0 .

On the profile curves of the menisci $f(y)$, it is necessary to satisfy the condition

$$V_{1n} = 0, \quad (12)$$

i.e., the condition of zero leakage, and the condition of absence of tangential stresses on the curves

$$[(\boldsymbol{\tau}, DV_1), \mathbf{n}] = 0, \quad x = f(y), \quad (13)$$

where D is the deformation rate tensor, which is equal to

$$DV_1 = \begin{pmatrix} \frac{\partial u_1}{\partial x} & \frac{1}{2} \left(\frac{\partial u_1}{\partial y} + \frac{\partial v_1}{\partial x} \right) \\ \frac{1}{2} \left(\frac{\partial u_1}{\partial y} + \frac{\partial v_1}{\partial x} \right) & \frac{\partial v_1}{\partial y} \end{pmatrix},$$

while \mathbf{n} and $\boldsymbol{\tau}$ are the normal and tangent vectors.

On the shaper edges, the condition of adhesion of the melt is satisfied

$$u_1 = 0, \quad v_1 = 0, \quad (x, y) \in \Gamma_1 \cup \Gamma_3, \quad (14)$$

and at the exit from the capillary channel

$$u_1 = 0, \quad v_1 = AV_0 \left[1 - \left(\frac{x}{d_0} \right)^2 \right], \quad (x, y) \in \Gamma_2, \quad (15)$$

where the constant A is determined from the condition of equality of the melt flows through the capillary channel and through the crystallization front:

$$A = \frac{3}{4d_0} \int_{-h_1}^{h_2} (1 + H^2(x)) dx.$$

We will consider the radiation heat exchange between plates in a cavity that is limited by two neighboring side surfaces of the strips by the segment of the x axis between the shapers and the segment of the straight line between the upper ends of the strips. Since the height of the melt meniscus is small compared to the strip length L and to the distance between the plates, the heat exchange of the liquid phase can be neglected.

The side surfaces of the crystal strips will be considered to be diffusely gray, so that a portion of the radiation $q_{i,k}(r_k)$ incident on the side surfaces of the crystal strips will be reflected and uniformly distributed in all directions at any point of the surface boundary. Then the reflected radiation and self-radiation can be combined into one effective radiation. We denote the flux densities q in the following manner: with the subscript i it refers to the incident radiation, with the subscript 0, to the effective radiation; the subscripts j and k characterize the properties of the j th and k th surfaces.

The resultant-flux density $q_k(r_k)$ for the areas elements of the surface of two neighboring strips that are described by the radius vectors r_k is reduced to the form:

$$q_k(r_k) = q_{0,k}(r_k) - q_{i,k}(r_k), \quad k = 1, 2. \quad (16)$$

The flux of effective radiation consists of the fluxes of self-radiation and reflected radiation:

$$q_{0,k}(r_k) = \varepsilon_k \sigma T_k^4(r_k) + (1 - \varepsilon_k) q_{i,k}(r_k). \quad (17)$$

The method of "balance" [1] makes it possible to write the following system of integral equations for determining the effective radiations $q_{0,k}(r_k)$:

$$q_{0,1}(y) - (1 - \varepsilon) \frac{1}{2} \int_0^L q_{0,2}(x) \frac{b^2}{[(x-y)^2 + b^2]^{3/2}} dx = \sigma (\varepsilon T_1^4(y) + (1 - \varepsilon) T_R^4), \quad (18)$$

$$q_{0,2}(y) - (1 - \varepsilon) \frac{1}{2} \int_0^L q_{0,1}(x) \frac{b^2}{[(x-y)^2 + b^2]^{3/2}} dx = \sigma (\varepsilon T_2^A(y) + (1 - \varepsilon) T_R^A), \quad (19)$$

where

$$T_R^A = T_s^A \frac{1}{2} \left[1 - \frac{y}{\sqrt{y^2 + b^2}} \right], \quad b = d + 2a - h_1^{(2)} - h_2^{(1)},$$

and T_s is the known surface temperature of the common base between the two neighboring shapers, while $h_2^{(1)}$ and $h_1^{(2)}$ are the quantities that are counted off from the y axis to the side adjacent surfaces of the neighboring strips; d is the distance between the shapers.

After determination of $q_{0,1}$ and $q_{0,2}$, we find the distributions of the resultant radiation fluxes q_1 and q_2 :

$$q_k(y) = \frac{\varepsilon}{1 - \varepsilon} [\sigma T_k^A(y) - q_{0,k}(y)], \quad (20)$$

or, by using the incident fluxes $q_{i,k}$, we find that

$$q_k(y) = \varepsilon [\sigma T_k^A(y) - q_{0,k}(y)] = \varepsilon \sigma (T_k^A - T_{enk}^A), \quad (21)$$

where

$$T_{enk}^A = \sqrt[4]{q_{i,k}/\sigma}, \quad k = 1, 2, \quad (22)$$

i.e., we obtain a radiation law which is similar to (5) but with other temperatures of the environments T_{enk} .

Let us introduce the stress function F according to the formulas

$$\sigma_x = \frac{\partial^2 F}{\partial y^2}, \quad \sigma_y = \frac{\partial^2 F}{\partial x^2}, \quad \sigma_{xy} = \frac{\partial^2 F}{\partial x \partial y}, \quad (23)$$

in which σ_x and σ_y are the normal stresses, while σ_{xy} are the tangential stresses.

In the case of the plane-stressed state the function F satisfies the equation

$$\Delta^2 F = -\frac{E}{1 - \nu} \alpha_t \Delta T_2, \quad (x, y) \in D_2, \quad (24)$$

where T_2 is the temperature distribution in the strip.

Proceeding from the requirement on the absence of surface forces, we formulate the boundary conditions

$$F = 0, \quad \frac{\partial F}{\partial n} = 0. \quad (25)$$

In the case of plane deformation, we have the normal stress σ_z that is related to the normal stresses acting over the other axes:

$$\sigma_z = \nu (\sigma_x + \sigma_y) - \alpha_t E T_2. \quad (26)$$

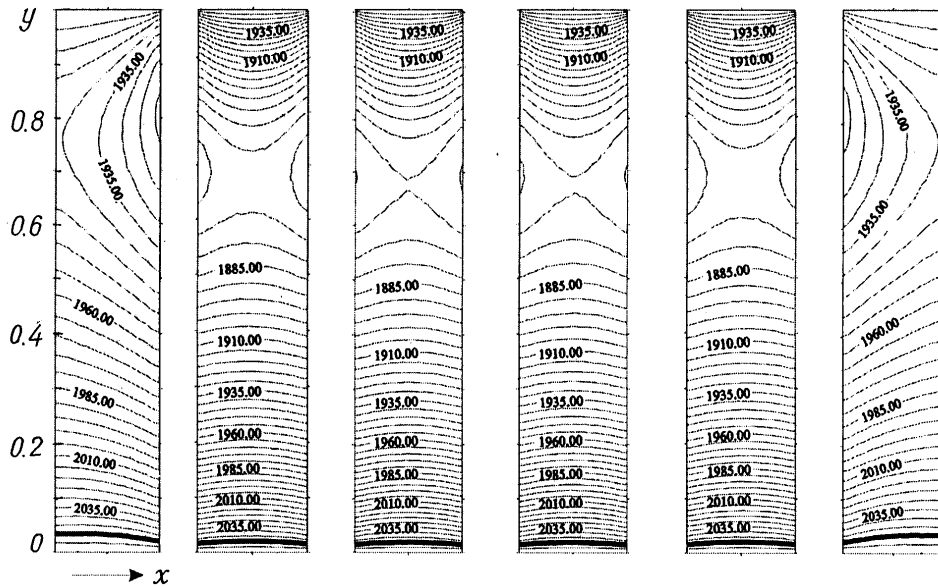


Fig. 2. Temperature fields in packet strips. $N = 6$, $L = 1$ cm, $2a = 0.2$ cm, $d = 0.25$ cm, $d_0 = 0.03$ cm, $T_1 = 2060^\circ\text{C}$, $T_2 = 1960^\circ\text{C}$, $T_{\text{en1}} = 2030^\circ\text{C}$, and $V_0 = 1.2$ mm/min. y , x , cm.

Since the stresses are absent on the upper end surface of the crystal, according to the St. Venant principle the temperature stresses over the z axis can be found from the expression

$$\sigma'_z = E\varepsilon_z + \sigma_z. \quad (27)$$

The constant deformation ε_z is determined as

$$\varepsilon_z = -\frac{1}{E |D_2|} \int_{D_2} \sigma_z dx dy, \quad (28)$$

where $|D_2|$ is the area of the region D_2 .

The solution of the heat problem (1)–(22) discussed above is given in [2]. This problem, just as the problem of finding thermoelastic stresses (23)–(28), was solved by the finite-element method [3].

Numerical Analysis and Discussion of the Results. In calculating the packet of six strips, we used the following data that corresponded to the experimental data, namely: the temperature of the operating surfaces of the shapers, comprising a single device for a group process, was taken to be identical for all the shapers and was equal to 2060 and 2055°C for different calculated variants; the temperature of the melt at the exit from the capillary channels of the shapers was equal to the temperature of the operating surfaces of the shapers. The temperature of the upper ends of the crystals of the packet was prescribed with account for the grown length in such a way that the temperature drop between them and the surface of the shapers was 100°C/cm. The temperature of the surrounding medium was prescribed in the form of the linear function

$$T_{\text{en}}(y) = T_{\text{en1}} - \tau y, \quad \tau = 70^\circ\text{C/cm}, \quad (29)$$

where $T_{\text{en1}} = 2030$ and 1850°C are the temperatures of the surrounding medium on the horizontal of the shapers (two variants).

Figure 2 presents typical temperature fields for the above-indicated temperature conditions; the crystallization fronts obtained in the calculation are denoted by the heavier line. It should be noted that the most

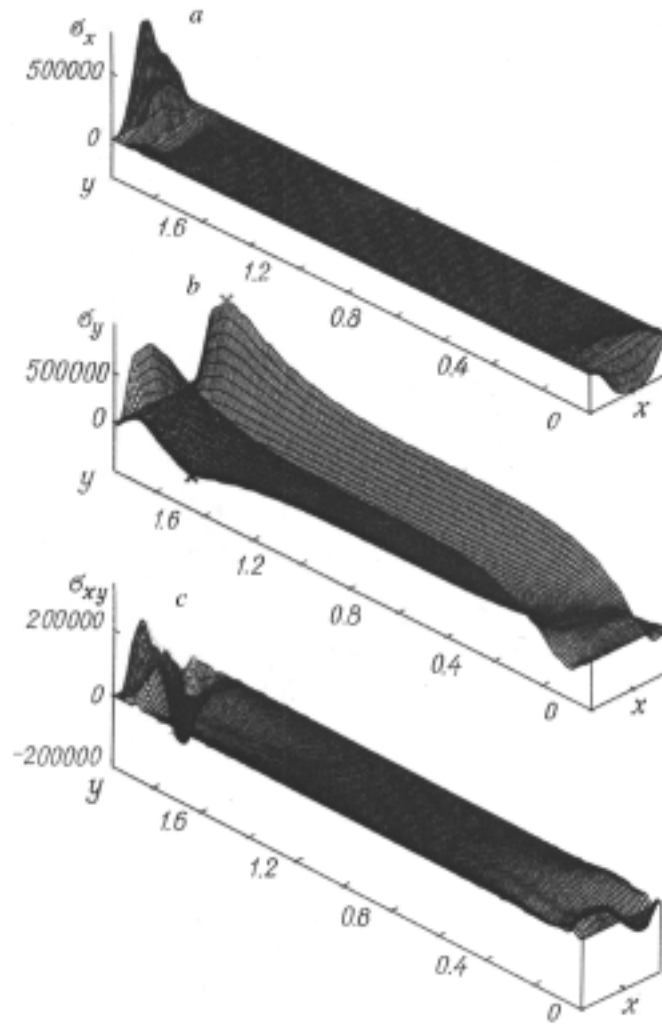


Fig. 3. Typical fields of the thermoelastic stresses in the outer packet strip of $L = 2$ cm. The remaining parameters are the same as in Fig. 2. σ , Pa.

significant changes in the thermal field, the meniscus height, and the shape of the interphase boundary occur in passage from the outer to the next strip of the packet, while the thermal fields, the heights, and the shapes of the fronts of the inner strips are virtually identical. This means that the outer strips are a kind of thermal shield for the inner strips.

The typical fields of the thermoelastic stresses of the outer strip of the packet σ_x , σ_y , and σ_{xy} are presented in Fig. 3. In this case, the maximum of the value of σ_x is positive; it is attained near the crystallization front and is slightly shifted to the outside of the strip due to the thermal field asymmetry. The minimum value turns out to be negative; it is attained at the upper end of the strip and is also shifted to the outside. In the remaining region, the stresses are virtually absent.

The stress σ_y is maximum (positive value) on the inner side surface of the strip and is attained at a distance of 1.61 mm from the crystallization front, while it is minimum (negative value) in the central region of the vertical section of the strip at a distance of 1.86 mm from the interphase boundary. Thus, the transition from the extension state to the compression state occurs in a small zone. The level of stresses decreases over the length of the strip and increases near its upper end, where the crystal is exposed to compression.

The tangential stress σ_{xy} is 5–7 times lower than normal stresses and attains extreme values near the crystallization front as well; then it is virtually absent and undergoes a slight increase in absolute value not

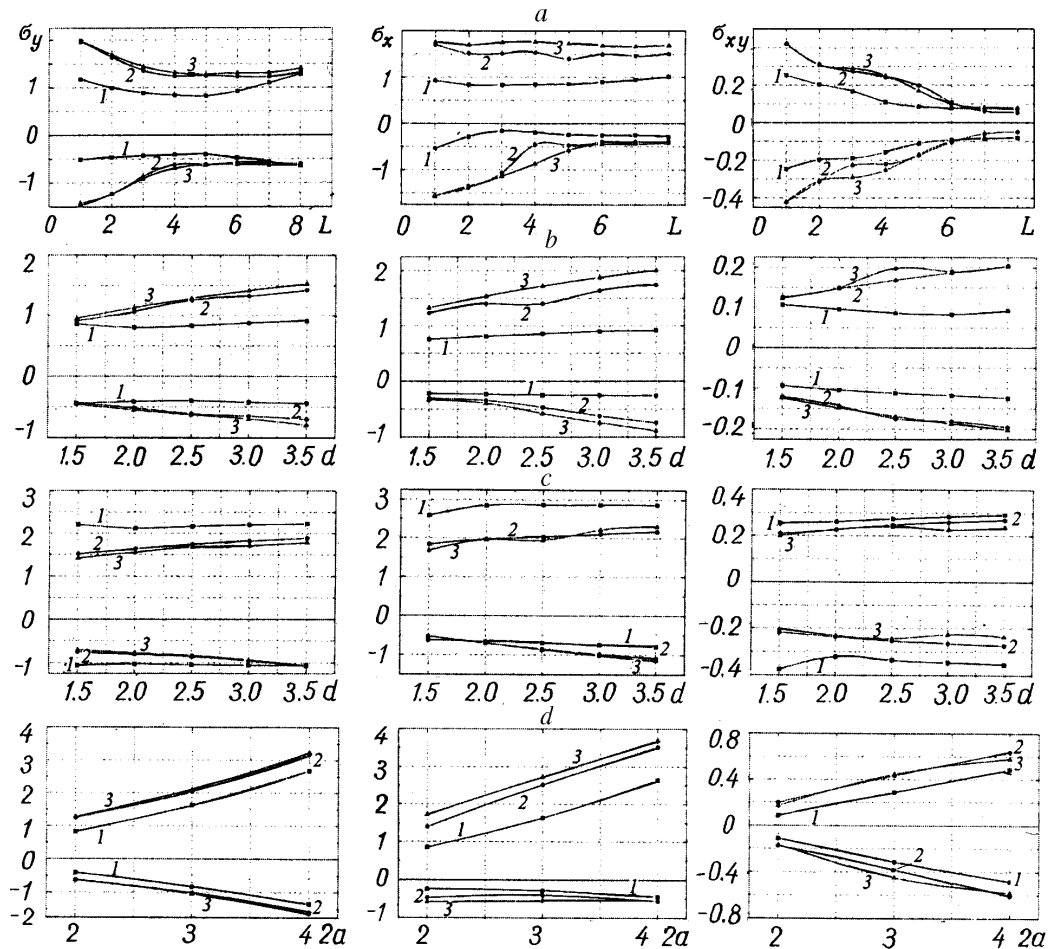


Fig. 4. Dependence of the maximum and minimum stresses in packet strips [1] the outer packet strip; 2, 3) the inner packet strips): a) on the length grown ($N = 6$, $2a = 0.2$ cm, $d = 0.25$ cm, $d_0 = 0.03$ cm, $T_1 = 2060^\circ\text{C}$, $T_{\text{enl}} = 2030^\circ\text{C}$, and $V_0 = 1.2$ mm/min); b) on the distance between the shapers ($N = 6$, $L = 5$ cm, $2a = 0.2$ cm, $d_0 = 0.03$ cm, $T_1 = 2060^\circ\text{C}$, $T_{\text{enl}} = 2030^\circ\text{C}$, and $V_0 = 1.2$ mm/min); c) on the distance between the shapers ($N = 6$, $L = 5$ cm, $2a = 0.2$ cm, $d_0 = 0.03$ cm, $T_1 = 2060^\circ\text{C}$, $T_{\text{enl}} = 1850^\circ\text{C}$, and $V_0 = 1.2$ mm/min); d) on the thickness of the shapers ($N = 6$, $L = 5$ cm, $d_0 = 0.03$ cm, $T_1 = 2060^\circ\text{C}$, $T_{\text{enl}} = 2030^\circ\text{C}$, and $V_0 = 1.2$ mm/min). σ , MPa; L , cm; d , $2a$, mm.

far from the upper end of the strip. It should be noted that the coordinates of the maximum and the minimum depend on the temperature drop over the heat zone and on the length of the strip grown at a given moment and on its position in the packet.

From the practical viewpoint, for high-quality single crystals to be produced, it is necessary to study the influence of the following factors on the thermoelastic stresses appearing in the plates: the temperature of the surrounding medium and the operating surface of the shaper, the length of the grown packet, and the geometric characteristics of the shaping device: the distance between separate neighboring shapers comprising a single device for a group process of growth, their transverse dimension, and the size of capillary channels. The final objective of the investigation is to select conditions for the crystallization process such that the maximum temperature stresses in the packet strips do not exceed the critical temperatures. To study these

dependences, it is convenient to use the quantities that represent the maximum and minimum values of the stresses considered, namely, σ_x , σ_y , and σ_{xy} .

The results of calculations of the maximum and minimum of the thermoelastic stresses for $T_{en1} = 2030^\circ\text{C}$ as functions of the length of the growing packet are presented in Fig. 4a. The highest and lowest stresses are attained at small lengths of the grown packet; the level of stresses in the inner packet strips is much higher than in the outer packet strips. The values of the stresses in the inner strips are virtually identical. In the course of growth, the equalization of the stress level is observed in all the packet strips.

With decrease in the distance between the neighboring shapers of the unit, the stress level in the outer and inner packet strips drops (Fig. 4b).

Next, we calculated the values of the thermoelastic stresses in the packet strips for a $T_{en1} = 1850^\circ\text{C}$ for a fixed length of the packet strips, equal to 5 cm, and a thickness of the shapers equal to 0.2 cm. The distance between the neighboring shapers was varied. The calculation results are given in Fig. 4c. In this case, the highest and lowest stresses are attained in the outer packet strips, during which the stress level in all the packet strips is considerably higher than for $T_{en1} = 2030^\circ\text{C}$. It should be noted that when $T_{en1} = 1850^\circ\text{C}$, the decrease in the distance between the shapers does not lead to a substantial drop of in the stresses in the packet strips.

The increase in the thicknesses of the shapers (packet strips) results in an increase in stress (Fig. 4d). The calculations have shown that with $h = 4$ mm and an insignificant decrease in the environment temperature (by 30°C) the stress level exceeds the critical one, which for the temperatures considered in the case of sapphire is 5 MPa.

Thus, an increase in the initial environment temperature T_{en1} for a constant gradient of the heat zone in combination with a decrease in the distance between the shapers makes it possible to substantially reduce the level of thermoelastic stresses in the packet strips.

The calculations have shown that a decrease in the temperature of the operating shaper surface by 5°C (from 2060 to 2055°C) causes an increase of almost 50% in the normal stress σ_x for both the outer and inner packet strips (for example, for the outer strip of thickness 1.87 mm the stress increases from 0.8 to 1.2 MPa). The value of the normal stress σ_y remains constant.

A decrease in the width of the capillary channel (from 0.6 to 0.3 mm) leads to an increase in the level of the tangential stresses σ_{xy} (from 0.1 to 0.15 MPa); the normal stresses remain virtually constant.

CONCLUSIONS

1. Based on the suggested mathematical model of the packet process of growth of crystal strips and on the calculations performed by this model, it is shown that the most significant parameters of the process are the temperature of the surrounding medium, the temperature of the operating shaper surface, and the distance between neighboring shapers.

2. The results given above point out the trend in optimizing the design of a shaper and the heat zone.

NOTATION

ρ_1 , density; c_i , specific heat; k_i , thermal conductivity coefficient; V_0 , pulling speed of the crystal; ΔH_f , specific heat of crystallization; h_G , heat-transfer coefficient; σ , Stefan–Boltzmann constant; ϵ , emissivity; g , free-fall acceleration; σ_{LG} , coefficient of surface tension of the melt; ϵ_0 , growth angle; H_{eff} , distance between the melt surface in a crucible and the line of the meniscus base; μ , dynamic viscosity of the melt; d_0 , half-width of the capillary channel; a , shaper half-thickness; d , distance between neighboring shapers; ν , Poisson coefficient; α_r , thermal-expansion coefficient; E , Young modulus; L , length of the packet strips; N , number of strips in the packet; T^0 , initial temperature of the surrounding medium on the horizontal of the shapers.

Subscripts: n and τ , normal and tangential components of anything; LG, characteristics of the quantity in passage from the liquid (L) to the gaseous medium (G); eff, effective quantity; G_i , radiation to the gaseous medium, with $i = 1$, from the meniscus surface, with $i = 2$, from the side surface of the crystal; m , refers to the melting temperature; x and y , distribution of anything in the direction of the x and y axes; en, environment.

REFERENCES

1. E. Mitchell and R. White, *Finite-Element Method for Partial Differential Equations* [Russian translation], Moscow (1981).
2. A. V. Borodin, A. V. Zhdanov, L. P. Nikolaeva, and I. S. Pet'kov, *Izv. Ross. Akad. Nauk, Ser. Fiz.*, **9**, 1719–1731 (1999).
3. R. Siegel and J. Howell, *Radiation Heat Exchange* [Russian translation], Moscow (1975).